

# Novel *Staphylococcus aureus* Secreted Protein Alters Keratinocyte Proliferation and Elicits a Proinflammatory Response *In Vitro* and *In Vivo*

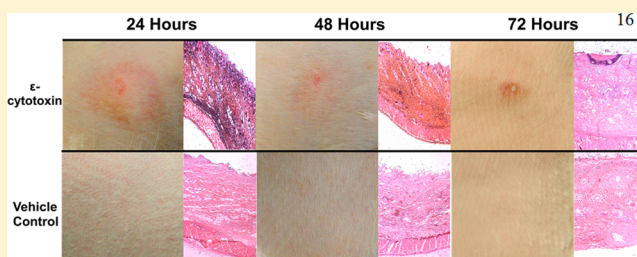
Joseph A. Merriman,<sup>†</sup> Aloysius J. Klingelutz,<sup>†</sup> Daniel J. Diekema,<sup>‡</sup> Donald Y. M. Leung,<sup>§</sup> and Patrick M. Schlievert<sup>\*,†</sup>

<sup>†</sup>Department of Microbiology, <sup>‡</sup>Division of Infectious Disease, University of Iowa, Iowa City, Iowa 52242, United States

<sup>§</sup>University of Colorado, Denver, Anschutz Medical Campus, Aurora, Colorado 80045, United States

## S Supporting Information

**ABSTRACT:** *Staphylococcus aureus* is a leading cause of surgical site infections that results in increased hospital stays due to the development of chronic wounds. Little is known about factors involved in *S. aureus*' ability to prevent wounds from healing. We discovered a novel secreted protein produced by a surgical site isolate of *S. aureus* that prevents keratinocyte proliferation. The protein has a molecular weight of 15.7 kDa and an isoelectric point of 8.9. The cloned and purified protein has cytotoxic and proinflammatory properties, as shown *in vitro* and *in vivo*. Potent biological effects on keratinocytes and rabbit skin suggest that this protein may play an important role in preventing re-epithelialization. Its lack of homology to known exotoxins suggests that this protein is novel, and this observation is likely to open a new field of research in *S. aureus* exotoxins. Due to its cytotoxic activities, we call this new protein *ε*-cytotoxin.



Annually, surgical site infections (SSIs) account for 17% of hospital-associated infections in the United States. SSIs are second only to catheter-associated urinary tract infections in the US.<sup>1</sup> SSIs occur in approximately 1% of surgeries, resulting in a yearly estimated 1 million extra days of hospital stays.<sup>2</sup> This increased length of hospitalization burdens the healthcare system with billions of dollars per year and is growing with the emergence of difficult-to-treat infecting pathogens.<sup>2,3</sup> SSIs can also progress to more serious infections such as sepsis or pneumonia.<sup>4</sup> *Staphylococcus aureus* is the most frequently (25–50%) isolated pathogen from SSIs, with the most common reservoir (80%) being patient nares.<sup>5</sup>

*S. aureus* is a multifaceted pathogen, capable of producing an array of virulence factors. These include microbial surface components recognizing adhesive matrix molecules (MSCRAMMs), other cell-surface virulence factors, such as protein A, and many secreted exoproteins, including superantigens, cytotoxins, and proteases. These virulence factors are tightly regulated as a function of bacterial growth phase.<sup>6–8</sup>

Previous research has shown that superantigens elicit cytokine responses from IFN- $\gamma$ -induced keratinocytes.<sup>9</sup> A potent proinflammatory and cytotoxic homoheptamer pore-former,  $\alpha$ -toxin, kills keratinocytes through membrane permeabilization.<sup>10</sup> Planktonic and biofilm conditioned media prevent scratch closure of keratinocytes *in vitro* as well as prevent wound closure in both murine and rabbit models, respectively.<sup>11–13</sup> Taken together, these data support *S. aureus*

secreted factors as being important mediators of impaired skin repair.

Keratinocytes are the major cell type of the epidermis and are responsible for maintaining tight physical barriers to biological and chemical threats. Keratinocytes are increasingly recognized as important immunological defenses in conjunction with physical barrier protection. Upon damage to the epidermis, keratinocyte cell–cell contact is disrupted and depends on cytokine production to initiate protective measures. Upon barrier disruption, active proliferation of keratinocytes is critical to epidermal reconstruction and, when inhibited, can result in chronic nonhealing wounds observed in SSIs.<sup>14</sup>

Insights into mechanisms of *S. aureus* prevention of wound closure are limited to examination of biofilm and planktonic conditioned media and their effects on keratinocyte monolayers. While these studies have demonstrated critical non-healing properties observed *in vivo*, they do little to identify critical factors or potential therapeutic targets involved in delayed healing.

A recent study dissecting the secretome of *S. aureus* estimates that ~50% of secreted *S. aureus* proteins are not functionally identified.<sup>15</sup> Bearing this in mind, we conducted an intensive study to fractionate and identify critical factors involved in *S. aureus*' ability to inhibit keratinocyte proliferation. Through the

Received: May 13, 2015

Revised: June 26, 2015

Published: July 15, 2015



use of a newly developed model of delayed confluence and mass spectrometry, we identified a novel protein, 15.7 kDa in molecular mass, capable of preventing keratinocyte proliferation. Extensive BLAST search, both of DNA and protein sequences, reveal conservation of this newly identified secreted protein across sequenced *S. aureus* strains, with the protein labeled as a conserved hypothetical secreted protein. No other similarities arise upon further dissection of the BLAST database, suggesting a novel activity of the hypothetical protein. This protein, when purified, demonstrates potent antiproliferative effects on keratinocytes as well as being cytotoxic and proinflammatory at higher concentrations to human keratinocytes. These diverse toxic activities led us to name this protein cytE, or  $\epsilon$ -cytotoxin.

## ■ EXPERIMENTAL PROCEDURES

**Pyrogens.** All glassware, reagents, and buffers used in these studies were maintained pyrogen-free. We have a long history of studies of bacterial pyrogenic toxin superantigens, lipopolysaccharides, and peptidoglycans as major pyrogens. These are excluded in our studies.

**Bacterial Strains and Isoelectric Focusing (IEF) Purification.** The Division of Infectious Diseases, University of Iowa, provided methicillin-resistant *S. aureus* (MRSA) surgical site strain 6 (SSI6). The strain was maintained in the Schlievert laboratory in the lyophilized state. Cultures were grown in beef heart dialysate medium at 37 °C with 225 rpm shaking for 48 h. One volume of culture (1200 mL) was poured into 4 volumes (4800 mL) of 100% ethanol to precipitate secreted exoproteins. The precipitates were pelleted at 4000g for 5 min. The pellet was resuspended at 1/10th volume in pyrogen-free distilled H<sub>2</sub>O and clarified by centrifugation (10 000g) for 30 min. The clarified supernate was dialyzed against 4 L of deionized water for 24 h using 12–14000 molecular weight cutoff dialysis tubing (Spectrum Laboratories, Inc., Rancho Dominguez, CA) and separated using preparative thin-layer IEF. Two successive IEFs with pH 3–10 ampholytes (Sigma-Aldrich, St. Louis, MO) allowed separation of major proteins; debris was removed from the first separation prior to re-IEF. The final thin-layer IEF plate was gridded into 15 fractions, which were harvested and each resuspended in 5 mL of pyrogen-free distilled H<sub>2</sub>O. Matrix Sephadex G75 superfine was removed from each fraction by filtration through glass wool and 0.45  $\mu$ m syringe filters (MilliporeEMD, Billerica, MD). Fractions were placed in dialysis tubing (6–8000 molecular weight cutoff) and dialyzed against 1 L of distilled water for 4 days, without water changes. Protein concentrations were subsequently determined using the Bradford assay (BioRad, Hercules, CA), with purified staphylococcal enterotoxin B as a protein standard. Fractions were both tested for delaying confluence of keratinocytes and submitted for mass spectrometry for protein identification.

**Tissue Culture.** TERT-immortalized adult skin keratinocytes, created by Dr. Aloysius Klingelutz, were cultured in keratinocyte serum-free medium (KSFM) (Gibco Life Technologies, Grand Island, NY) supplemented with bovine pituitary extract, recombinant epithelial growth factor (rEGF), 1% penicillin–streptomycin, and 1% fungizone at 37 °C in 5% CO<sub>2</sub>. These cells have previously been shown to have properties in common with nonimmortalized human adult keratinocytes.<sup>16</sup> Twenty-four-well tissue culture plates (Costar/Corning, Corning, New York) were seeded with 50 000 keratinocytes/well, as determined by hemocytometer, and

allowed to adhere for 2 h. The medium was removed, and adhered cells were gently washed with prewarmed KSFM before adding KSFM + cytE concentrations to a final volume of 0.5 mL/well. Images were taken every 24 h up to 72 h using a Nikon SMZ 1500 at 60 $\times$  magnification with QImaging camera and accompanying QCapture software (QImaging, British Columbia, Canada). Images were captured at 1280  $\times$  960 resolution. Cells were counted from images using ImageJ (NIH) using a grid overlay of 15 170 pixels<sup>2</sup>. ImageJ cell counter was used to count individual cells in three 3  $\times$  3 grid (136 530 pixels<sup>2</sup>) patterns per picture, and the counts were averaged. All experiments were performed in duplicate for a total of 12 data points. Significance was calculated using a paired Student's *t* test with a *P*-value < 0.05 considered to be significant.

**Mass Spectrometry.** NanoLC-MS/MS with Orbitrap mass spectrometry was carried out on selected trypsin-digested fractions. MS/MS spectra were extracted from the raw data files using msconvert ([proteowizard.sourceforge.net](http://proteowizard.sourceforge.net)) to generate input search files for assigning peptide sequence to tandem mass spectra. The UniProt/Swiss-Prot Staph aureus database (10 110 entries) and the UniProt/TREMBL Staph aureus database (1 079 187 entries) were used. The MS2 spectra were searched using the MyriMatch search engine.<sup>17</sup> Peptide spectral matches were then qualified using IDPicker.<sup>18</sup> Proteins were matched at a false discovery rate of less than 0.03% with a two peptide match minimum. Results obtained from UniProt/Swiss-Prot and UniProt/TREMBL databases were filtered based on seven or more distinct peptides in each fraction using Venny.

**Cloning and Screening of Hypothetical Protein.** Signal sequence was determined *in silico* using SignalIP 4.1. The hypothetical protein gene, renamed by us to cytE, plus and minus putative signal sequence, was cloned into the pET28a vector (Novagen/MilliporeEMD Billerica, MD) with use of primers outlined in Supporting Information Table S1 to attach an amino- or carboxy-terminal His-Tag. Protein was expressed in BL21 *Escherichia coli* (Invitrogen Life Technologies, Grand Island, NY) seeded in terrific broth (TB) + 50  $\mu$ g/mL kanamycin to a final OD<sub>600</sub> of 0.05 and shaken at 225 rpm to aerate at 30 °C for 2 h. A final concentration of 0.5 mM isopropyl  $\beta$ -D-1-thiogalactopyranoside (IPTG) (RPI, Mount Prospect, IL) was added, and cultures continued growth at 30 °C for 18 h to induce protein production. Protein was released from cells through sonication and purified using batch purification (>90% purity) through the use of cobalt-linked agarose resin (Sigma, St. Louis, MO). Protein was eluted in a Tris-buffered solution containing 500 mM imidazole followed by dialysis in 6–8000 molecular weight cutoff dialysis tubing against 1 L of pyrogen-free distilled H<sub>2</sub>O for 24 h. Protein concentration was determined via the Bradford reagent using staphylococcal enterotoxin B as a standard. The hypothetical protein was screened for in *S. aureus* strains, using Phusion polymerase (New England Biosciences, Ipswich, MD), with the primers  $\epsilon$ -toxFwd 5'-GTACTTGTTACACGTAAAGATAG-3' and  $\epsilon$ -toxRev 5'-TTATTCTTTATCAGATAATGCATTTT-3'.

**Cytotoxicity and IL-8 Enzyme-Linked Immunosorbent Assay.** Keratinocytes were grown to confluence in 96-well tissue culture plates. Twenty-four hours prior to experimentation, KSFM without antibiotic was added. Test protein was added in specified amounts and incubated with cells for 6–24 h. Post 6 and 24 h, supernates were removed, and IL-8 was quantified using IL-8 Quantikine ELISA (R&D Systems,

Minneapolis, MN). Cells were coincubated with fresh KSFM and CellTiter 96 AQueous One Solution (Promega, Madison, WI) (20  $\mu$ L/100  $\mu$ L media; 120  $\mu$ L mixture/well) for 1 h. Absorbance was taken at 490 nm wavelength with use of a Tecan Infinite 200 Pro microplate reader. All experiments were performed in triplicate. Lysis of human and rabbit red blood cells (RBCs) was measured after placing RBCs in agarose.<sup>19</sup> Paired two-tailed Student's *t* test was used, with *P* < 0.05 considered to be significant.

**Rabbit Subcutaneous, Intravenous Injection, and Polyclonal Antibody Generation.** New Zealand white, 4–5 lbs, mixed sex rabbits were used in accordance under an approved University of Iowa IACUC protocol. Briefly, rabbit right and left flanks were shaved using an electric clipper. Subcutaneous injection of 135  $\mu$ g/100  $\mu$ L of recombinant His- $\epsilon$ -cytotoxin or bovine serum albumin (BSA) was performed on opposite flanks of the animal. Vehicle (100  $\mu$ L), as a control, was also injected subcutaneously on same flank as BSA control. Inflammation was observed via pictures and histology at each time point. Diameter of inflammatory regions, as demarked by reddening/raising of skin around injection site, was measured in millimeters using a standard ruler. Data were collected every 24 h up to 72 h. Significance was calculated using a paired two-tailed Student's *t* test, with a *P*-value < 0.05 considered to be significant. Intravenous injections were performed by administration of 135  $\mu$ g of toxin or buffer, brought up to a total volume of 1 mL in phosphate buffered saline (PBS), into the marginal ear veins. Temperatures were measured rectally every hour for 4 h. At the end of each experiment, rabbits were euthanized and observed for gross pathological changes to internal viscera. Immunization protocol to generate polyclonal antibody in rabbits was generated as previously described.<sup>20</sup> Significance was calculated using a two-way ANOVA test, with a *P*-value < 0.05 considered to be significant.

## RESULTS

***S. aureus* SSI6 Supernate Prevents Keratinocyte Confluence.** The University of Iowa Division of Infectious Disease provided a MRSA surgical site infection strain 6 (SSI6). Ethanol concentrated culture and filtered supernate was prepared from an overnight culture of SSI6. Ethanol concentrated culture and filtered supernate were tested in the delayed confluence assay. Both ethanol concentrates and supernate were capable of significantly (*P* < 0.05) preventing keratinocyte proliferation at all total protein concentrations tested, 40–400  $\mu$ g/mL (data not shown), compared to PBS control.

Our standard protocol for IEF purification<sup>21</sup> was performed on ethanol concentrated SSI6 culture. Of the 15 fractions obtained, fractions 7–14 had significant inhibitory effects on keratinocyte proliferation. Approximately 60  $\mu$ g/mL of total protein in fractions 7–14 displayed significant (at least *P* < 0.05) ability to prevent keratinocyte proliferation when compared to PBS control over the 72 h test period (Figure 1a,b).

**Mass Spectrometry Identified a Single Novel Hypothetical Secreted Protein, Tentatively Named  $\epsilon$ -Cytotoxin, from UniProt/Swiss-Prot and UniProt/TREMBL Databases.** Fractions 7, 9, 11, 14, and 15 were selected for mass spectrometry based on conserved bands in SDS-PAGE (Supporting Information Figure S1) and their ability to delay confluence (Figure 1). These fractions were subjected to trypsin digestion and subsequent nanoLC-MS/MS with

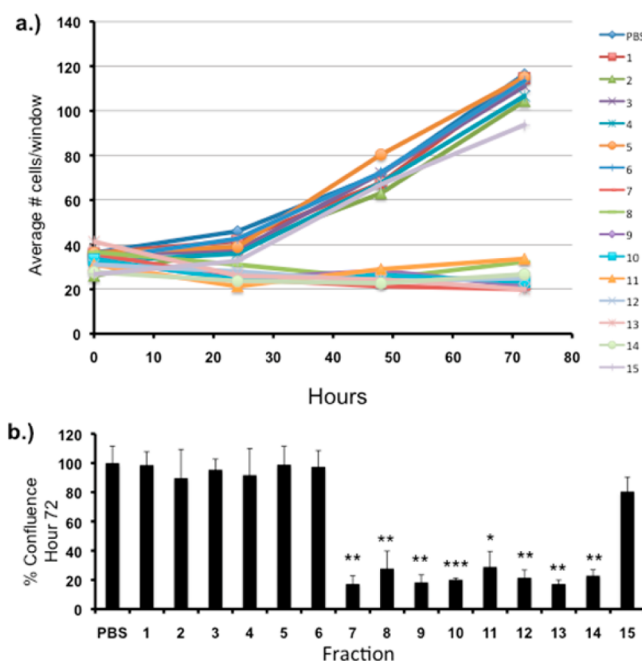


**Figure 1.** Secreted factors differentially impact keratinocytes ability to reach confluence. (a) Isoelectric focusing fractions 7–14 prevented keratinocyte proliferation over 72 h, as noted by the average number of cells counted in each well of a delayed confluence assay. (b) Level of keratinocyte confluence was significantly (at least *P* < 0.05) lower in fractions 7–14 after 72 h.

Orbitrap mass spectrometry. Fractions 7, 9, 11, and 14 were individually compared to fraction 15, which lacked activity, using a five distinct peptide cutoff limit. Remaining hits were compared using Venny, an online Venn diagram program, and conserved proteins found in all fractions except 15 were identified. This process yielded one unique hit, appearing as 114 redundant entries, classified as hypothetical secreted protein (Figure 2a). The highest number of peptides, 16, as well as percent coverage, 80.7%, of this hypothetical secreted protein was in fraction 14. Twelve distinct peptides, 74.3% coverage, were found in fraction 11. Ten distinct peptides were observed in fractions 9 and 7 (52.1 and 44.3% coverage, respectively). Only five distinct peptides were found in fraction 15 with only 40.7% coverage, supporting the focusing of this protein to fraction 14.

Hypothetical protein sequence BLAST returned hits in many *S. aureus* strains at >99% homology. Published sequences of other staphylococcal species, *S. simiae*, *S. pasteurii*, *S. caprae*, *S. warneri*, *S. capitis*, *S. epidermidis*, showed an amino acid homology range of 76–67% (Figure 2b). WebLogo 3.0 analyses of these sequences revealed a relatively conserved AXA signal peptidase cleavage motif at amino acids 12–15 (Figure 2c).  $\epsilon$ -Cytotoxin is labeled as a conserved hypothetical protein under *S. aureus* strain COL sequence annotated SACOL1802. The hypothetical protein sequence, when applied to Phyre2.0 protein modeling software, is returned with a modeling confidence of <16%, suggesting a highly novel structure unpredictable with current *in silico* methods.

**$\epsilon$ -Cytotoxin Is Core Genome-Encoded and Found Across Clinical and Lab-Adapted Strains.** Twenty-six clinical isolates, USA100–400s, and three common laboratory strains were tested for presence of  $\epsilon$ -cytotoxin gene. RN4220, RN450, and RN6390 are all strains used in the laboratory for

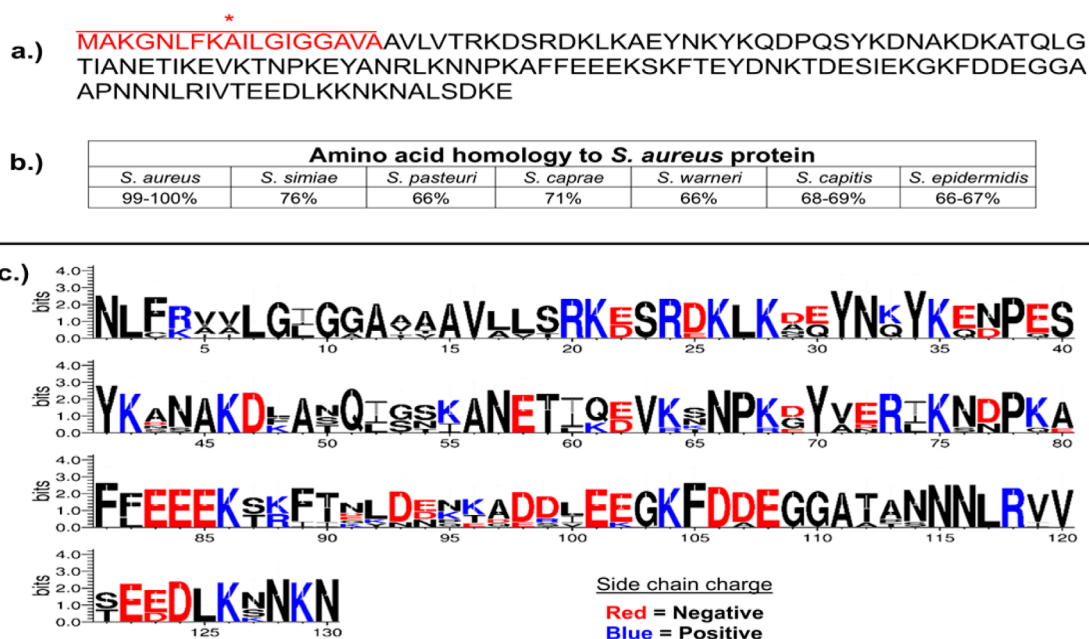


**Figure 2.** Unique, conserved hypothetical protein identified in active fractions. (a) Amino acid sequence of hypothetical protein,  $\epsilon$ -cytotoxin, with underlined and starred sequence denoting putative signal peptide identified by SignalIP 4.1 and removed in His-Tagged expression. (b) Amino acid homology of protein found in other staphylococci sequenced and in BLAST database. (c) WebLogo 3.0 shows relatively conserved signal peptide region with AXA signal peptidase recognition site as well as other conserved regions of  $\epsilon$ -cytotoxin, potentially important in activity.

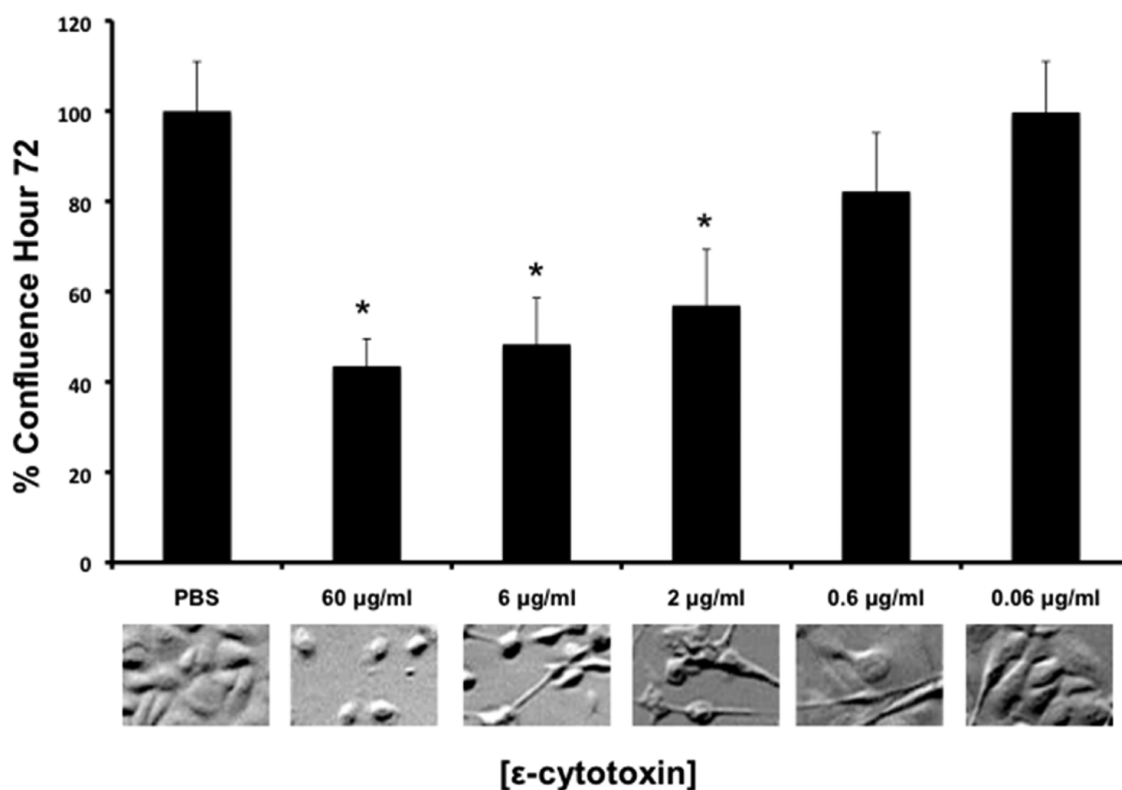


**Figure 3.**  $\epsilon$ -Cytotoxin causes significant proliferation inhibition and morphological changes in keratinocytes. Keratinocytes displayed a significant ( $P < 0.05$ ) delay in reaching confluence in the presence of  $\epsilon$ -cytotoxin at concentrations of 2–60  $\mu$ g/mL when compared to PBS control. Morphological alterations were seen across all tested concentrations (0.06–60  $\mu$ g/mL) and can occur independent of the delayed confluence phenotype ( $n = 3$  per challenge).

protein expression. All strains tested encoded for *cytE*, in conjunction with gene presence in available sequenced isolates (>3000 isolates), suggesting that  $\epsilon$ -cytotoxin is a core genome-encoded protein.

**Amino-Terminal His-Tagged, Cobalt-Purified  $\epsilon$ -Cytotoxin Lacking Putative Signal Sequence Is Stably Expressed and Capable of Inhibiting Keratinocyte Proliferation and Altering Cell Morphology.** The program

SignalIP 4.1 identified a putative signal sequence (MAKG-NLFKAILGIGGAVA) in  $\epsilon$ -cytotoxin (Figure 2a). All carboxy-terminal tagged proteins, with and without the putative signal sequence, caused the protein to be unstable and could not be purified. Amino-terminal-tagged protein with the putative signal sequence was also unstable (data not shown). Amino-terminal-tagged protein lacking the putative signal sequence was stably expressed and successfully purified to >95% homogeneity, as demonstrated by SDS-PAGE (Supporting Information Figure S2a). Generation of rabbit polyclonal antibody, using this protein preparation, allowed detection of the *S. aureus* produced version of this protein. Time course analysis was performed every hour for 8 h and again at 24 and 30 h. Western blot analysis revealed that protein production begins at approximately  $1.4 \times 10^9$  CFU/mL (postexponential phase) when grown in broth cultures (Supporting Information Figure S2b,c).

Purified His- $\epsilon$ -cytotoxin was capable of inhibiting keratinocyte proliferation. Compared to PBS control, concentrations of 2–60  $\mu$ g/mL of  $\epsilon$ -cytotoxin were significantly able to decrease the ability of keratinocytes to reach confluence. At all ranges of concentrations tested, 0.06–60  $\mu$ g/mL, cells showed abnormal cell morphology by hour 72 (Figure 3). Keratinocytes exposed to >60  $\mu$ g/mL of  $\epsilon$ -cytotoxin were observed to have a rounded cell morphology, typically seen in epithelial cell death *in vitro*, although keratinocytes remained attached to plates.

**Purified  $\epsilon$ -Cytotoxin Lyses RBCs, Is Cytotoxic to Keratinocytes, and Is Proinflammatory at Subcytotoxic Doses after 24 h Exposure.** Due to significant keratinocyte morphological changes observed during studies of delayed confluence (Figure 3), we hypothesized that cellular cytotoxicity may play a critical role in  $\epsilon$ -cytotoxin's interaction with host cells.  $\epsilon$ -Cytotoxin was hemolytic to rabbit RBCs when 12.5–25  $\mu$ g/20  $\mu$ L volume was exposed to RBCs in agarose (Supporting Information Figure S3).

We next investigated the ability of  $\epsilon$ -cytotoxin to kill keratinocytes by assaying production of NADH.  $\epsilon$ -Cytotoxin was acutely cytotoxic (6 h incubation) to keratinocytes at >25  $\mu$ g/mL, independent of IL-8 production (Supporting Information Figure S4). After 24 h exposure, >10  $\mu$ g/mL of  $\epsilon$ -cytotoxin was cytotoxic, with significant levels of IL-8 being produced at concentrations 10–20  $\mu$ g/mL (Figure 4a,b). At a concentration significant for delayed confluence,  $\geq 2$   $\mu$ g/mL (Figure 3), we saw no cytotoxicity or proinflammatory response, suggesting  $\epsilon$ -cytotoxin can alter keratinocyte proliferation, independent of cell death and inflammation.

**$\epsilon$ -Cytotoxin Is Proinflammatory When Injected Subcutaneously and Elicits Fever Responses When Administered Intravenously.** The cytotoxicity of  $\epsilon$ -cytotoxin, as seen *in vitro* (Figure 4a,b), led us to test  $\epsilon$ -cytotoxin's effects *in vivo*. In 100  $\mu$ L volumes, 135  $\mu$ g of toxin, bovine serum albumin (BSA), or vehicle control (Buffer B) were injected subcutaneously, monitored, and measured over a 72 h period for inflammation at the injection site (Figure 5a–j). Significant redness was observed around the toxin injection site after 24 h and persisted out to 48 h (Figure 5d,e). Histological observation of full-thickness skin sections indicated significant PMN infiltration after 24 h, with inflammation slowly resolving at hour 48. After 72 h, the majority of the redness surrounding the injection site had dissipated, leaving a dark, damaged area at the injection site (Figure 5f). None of these signs of inflammation were seen in either the BSA or vehicle control over the entire 72 h period (Figure 5a–c,g–i). Significant

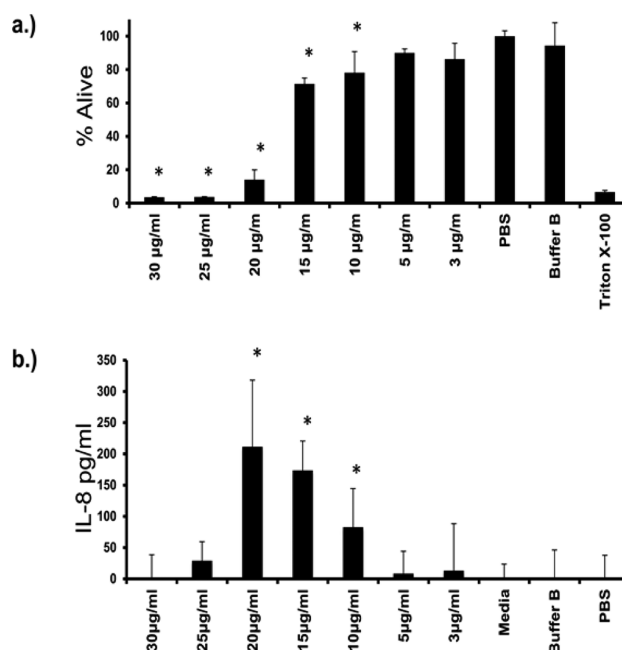


**Figure 4.**  $\epsilon$ -Cytotoxin is both cytotoxic and proinflammatory after 24 h exposure. (a)  $\epsilon$ -Cytotoxin was capable of significant ( $P < 0.05$ ) toxicity, as measured by NADH production, to keratinocytes at concentrations 10–30  $\mu$ g/mL. (b)  $\epsilon$ -Cytotoxin elicited a significant IL-8 response between 10 and 20  $\mu$ g/mL but not  $\geq 25$   $\mu$ g/mL due to acute toxicity killing cells before a proinflammatory response was generated. All experiments were done in triplicate.

swelling at the injections site, as monitored by the inflammation diameter, was observed in as little as 4 h after injection of toxin but not in BSA or vehicle control ( $P < 0.001$ ) (Figure 5j). The area of inflammation steadily declined over the 72 h period but remained significant ( $P = 0.028$ ) in sites injected with toxin (Figure 5).

To determine the systemic inflammatory capabilities of  $\epsilon$ -cytotoxin, rabbits were injected intravenously with 135  $\mu$ g of toxin or vehicle control, in 1 mL volumes of PBS. Rabbit temperature was monitored rectally over 4 h (Figure 6). We noted an increase in temperature of the three rabbits injected with  $\epsilon$ -cytotoxin over the 4 h period that was significantly ( $P = 0.0046$ ) higher than the vehicle control, as determined by two-way ANOVA.

## DISCUSSION

Surgical site infections are an ever-increasing burden on the healthcare system due to (1) their chronic nature and (2) the presence of difficult-to-treat infecting microbes.<sup>2</sup> *S. aureus*, a prominent nosocomial pathogen, is increasingly difficult to treat due to acquisition of antibiotic resistance coupled with lack of complete understanding of how the organism causes infections. Previous research has characterized some conditions, i.e., biofilm and planktonic growth, having differing degrees of both inflammation and ability to prevent wound healing.<sup>11–13</sup> However, these studies have done little to identify factors responsible for perpetuating chronic wounds.

In this study, we identified and characterized a novel protein conserved across clinical and laboratory-adapted strains of *S. aureus* capable of preventing both keratinocyte proliferation and ability to achieve confluence. A broad concentration range, 60 ng/mL to 60  $\mu$ g/mL, demonstrated the protein's ability to alter keratinocyte cell morphology as well. Preventing re-epithelial-

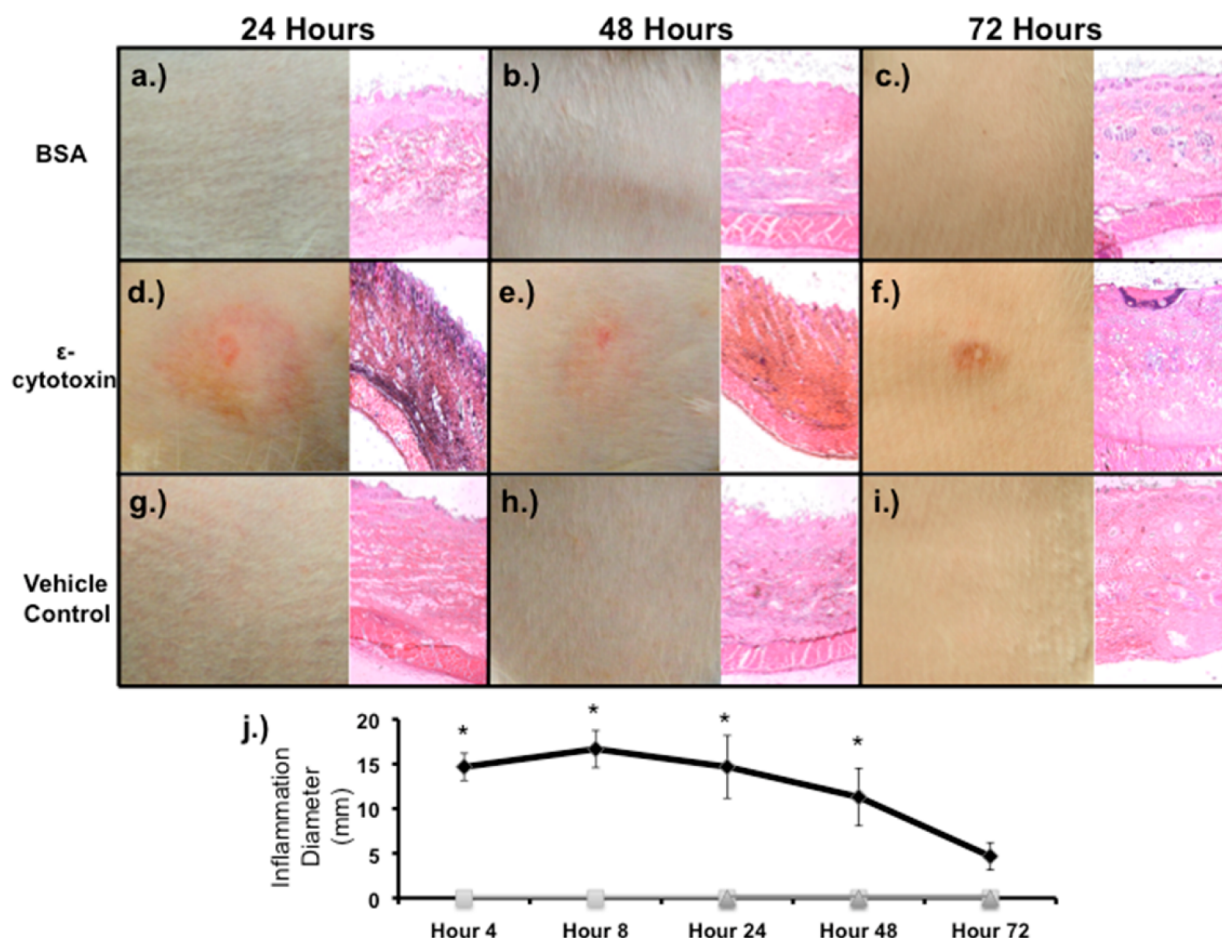


**Figure 5.** Subcutaneous injection of  $\epsilon$ -cytotoxin causes significant inflammation. Epidermis is the top of each histology section at 20 $\times$  magnification. Bovine serum albumin (p) (a–c) ( $n = 3$ ) and vehicle control (n) (g–i) ( $n = 3$ ) showed no inflammation over the 72 h period, with large nucleated cells appearing at 72 h (c, i), denoting anagen, the normal process of growing hair after shaving.  $\epsilon$ -Cytotoxin (u) ( $n = 3$ ) injection sites were significantly ( $P < 0.05$ ) inflamed in as little as 4 h (j), with significant inflammation and PMN infiltration after 24 h (e). Significant inflammation persisted over the 72 h period (e, f, j), with the host appearing to resolve the inflammation into a  $\sim 3$  mm necrotic lesion by 72 h (f).

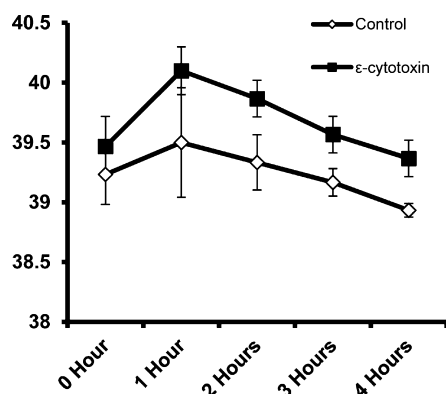


**Figure 6.** Significant fever response is elicited when rabbits are exposed to  $\epsilon$ -cytotoxin. Intravenous injection of  $\epsilon$ -cytotoxin (n) ( $n = 3$ ) or vehicle control (u) ( $n = 3$ ) shows  $\epsilon$ -cytotoxin significantly ( $P = 0.0046$ ) increased body temperature over the 4 h period when compared to vehicle control, as determined by two-way ANOVA.

ization is a crucial step in preventing wound healing, suggesting  $\epsilon$ -cytotoxin may play a critical role in *S. aureus* infected chronic wounds.

$\epsilon$ -Cytotoxin was cytotoxic to keratinocytes at concentrations  $\geq 10$   $\mu$ g/mL and was proinflammatory to keratinocytes at

concentrations of 10–20  $\mu$ g/mL. The cytotoxicity at early time points likely prevented measurable proinflammatory responses at later time points. While concentrations of 3–5  $\mu$ g/mL were not cytotoxic or proinflammatory to keratinocytes, we found that concentrations of  $\epsilon$ -cytotoxin as low as 2  $\mu$ g/mL were able to significantly delay keratinocyte proliferation. This suggests delayed re-epithelialization is still possible with minimal inflammation. Acute SSIs are typically highly inflamed, whereas chronic SSIs typically persist with low-level inflammation.<sup>13,22</sup> Our data indicate  $\epsilon$ -cytotoxin has a potential role in this delayed wound healing in a low-inflammatory environment.

To determine if the observed *in vitro* biological activities were also observed *in vivo*,  $\epsilon$ -cytotoxin was injected subcutaneously and intravenously into rabbits. We noted significant inflammation and swelling starting in as little as 4 h after initial injection of  $\epsilon$ -cytotoxin. Gross pathology and histology also demonstrated significant inflammation, as indicated by infiltration of PMNs into the epidermis after only 24 h. Further testing of  $\epsilon$ -cytotoxin at lower levels will need to be completed to determine its role in preventing wound closure.  $\epsilon$ -Cytotoxin was also inflammatory when injected intravenously, as measured by fever, suggesting that  $\epsilon$ -cytotoxin is able to exert proinflammatory effects both locally and systemically.

Many surgical site infections are considered to be biofilms, which can be difficult to eradicate with antibiotics and may

require debridement of infected areas.<sup>23</sup> Kinetics suggest that toxin expression occurs at similar times as that of other major exotoxins, i.e., late log and early stationary phases (Supporting Information Figure S1c), suggesting that  $\epsilon$ -cytotoxin is under regulatory control that is similar to that of other well-characterized virulence factors. Given its highly novel nature and significant effects *in vitro* and *in vivo*, it is likely that  $\epsilon$ -cytotoxin contributes to wound infections by preventing re-epithelialization and promoting dysregulation at the site of healing. Alternatively, the killing of keratinocytes and epithelial cells by  $\epsilon$ -cytotoxin could contribute indirectly to inflammation by causing production of danger signals through cytotoxicity.

$\epsilon$ -Cytotoxin is a protein with an estimated pI of 8.9, and it has a molecular size of 15.7 kDa. The protein appears to be chromosomally encoded, having a signal peptide for its secretion from *S. aureus*. The mechanism by which the protein is cytotoxic is unknown, and the protein does not have homology to the pore-forming staphylococcal cytotoxins. We have presented evidence suggesting the potential critical role of  $\epsilon$ -cytotoxin in *S. aureus* wound pathogenesis. Our findings warrant further investigation into its overall contribution to *S. aureus* virulence. The potency of  $\epsilon$ -cytotoxin, coupled with its novelty, may open a new field of research in staphylococcal virulence and may provide a new target for future immunization studies.

## ■ ASSOCIATED CONTENT

### ■ Supporting Information

Supplementary Figure 1 shows 16% SDS-PAGE Coomassie brilliant blue R-250 stained gels of SSI6 fractions separated by 3–10 pH isoelectric focusing. Supplementary Figure 2 shows the purification of recombinant protein and detection in SSI6 *S. aureus* strain. Supplementary Figure 3 shows pixel area, as determined by ImageJ (NIH), of blood lysis attributed to  $\epsilon$ -cytotoxin amounts in 5% sheep blood agar. Supplementary Figure 4 demonstrates the toxicity of  $\epsilon$ -cytotoxin at 6 hours post incubation on keratinocytes, as measured by NADH production. Supplementary Table 1 lists the primers used to generate recombinant  $\epsilon$ -cytotoxin used in this study. The Supporting Information is available free of charge on the ACS Publications website at DOI: 10.1021/acs.biochem.5b00523.

## ■ AUTHOR INFORMATION

### Corresponding Author

\*E-mail: [patrick-schlievert@uiowa.edu](mailto:patrick-schlievert@uiowa.edu). Tel.: 319-337-7807.

### Funding

This research was supported by grant 1 U19 AI117673-01 from the U.S. Public Health Service. Animal studies were supported by a University of Iowa start-up grant to P.M.S.

### Notes

The authors declare no competing financial interest.

## ■ REFERENCES

- (1) Perencevich, E. N.; Sands, K. E.; Cosgrove, S. E.; Guadagnoli, E.; Meara, E.; and Platt, R. (2003) Health and economic impact of surgical site infections diagnosed after hospital discharge. *Emerging Infect. Dis.* 9, 196–203.
- (2) de Lissovoy, G.; Fraeman, K.; Hutchins, V.; Murphy, D.; Song, D.; and Vaughn, B. B. (2009) Surgical site infection: incidence and impact on hospital utilization and treatment costs. *Am. J. Infect. Control* 37, 387–397.
- (3) Engemann, J. J.; Carmeli, Y.; Cosgrove, S. E.; Fowler, V. G.; Bronstein, M. Z.; Trivette, S. L.; Briggs, J. P.; Sexton, D. J.; and Kaye, K.

S. (2003) Adverse clinical and economic outcomes attributable to methicillin resistance among patients with *Staphylococcus aureus* surgical site infection. *Clin. Infect. Dis.* 36, 592–598.

(4) Cantlon, C. A.; Stemper, M. E.; Schwan, W. R.; Hoffman, M. A.; and Qutaishat, S. S. (2006) Significant pathogens isolated from surgical site infections at a community hospital in the Midwest. *Am. J. Infect. Control* 34, 526–529.

(5) von Eiff, C.; Kipp, F.; and Becker, K. (2002) Intranasal mupirocin to prevent postoperative infections. *N. Engl. J. Med.* 347, 1207–1208.

(6) Said-Salim, B.; Dunman, P. M.; McAleese, F. M.; Macapagal, D.; Murphy, E.; McNamara, P. J.; Arvidson, S.; Foster, T. J.; Projan, S. J.; and Kreiswirth, B. N. (2003) Global regulation of *Staphylococcus aureus* genes by Rot. *J. Bacteriol.* 185, 610–619.

(7) Pragman, A. A.; Yarwood, J. M.; Tripp, T. J.; and Schlievert, P. M. (2004) Characterization of virulence factor regulation by SrrAB, a two-component system in *Staphylococcus aureus*. *J. Bacteriol.* 186, 2430–2438.

(8) Voyich, J. M.; Vuong, C.; DeWald, M.; Nygaard, T. K.; Kocianova, S.; Griffith, S.; Jones, J.; Iverson, C.; Sturdevant, D. E.; Braughton, K. R.; Whitney, A. R.; Otto, M.; and DeLeo, F. R. (2009) The SaeR/S gene regulatory system is essential for innate immune evasion by *Staphylococcus aureus*. *J. Infect. Dis.* 199, 1698–1706.

(9) Nickoloff, B. J.; Mitra, R. S.; Green, J.; Shimizu, Y.; Thompson, C.; and Turka, L. A. (1993) Activated keratinocytes present bacterial-derived superantigens to T lymphocytes: relevance to psoriasis. *J. Dermatol. Sci.* 6, 127–133.

(10) Walev, I.; Martin, E.; Jonas, D.; Mohamadzadeh, M.; Muller-Klieser, W.; Kunz, L.; and Bhakdi, S. (1993) Staphylococcal alpha-toxin kills human keratinocytes by permeabilizing the plasma membrane for monovalent ions. *Infect. Immun.* 61, 4972–4979.

(11) Secor, P. R.; James, G. A.; Fleckman, P.; Olerud, J. E.; McInerney, K.; and Stewart, P. S. (2011) *Staphylococcus aureus* biofilm and planktonic cultures differentially impact gene expression, mapk phosphorylation, and cytokine production in human keratinocytes. *BMC Microbiol.* 11, 143.

(12) Kirker, K. R.; Secor, P. R.; James, G. A.; Fleckman, P.; Olerud, J. E.; and Stewart, P. S. (2009) Loss of viability and induction of apoptosis in human keratinocytes exposed to *Staphylococcus aureus* biofilms *in vitro*. *Wound Repair Regen* 17, 690–699.

(13) Gurjala, A. N.; Geringer, M. R.; Seth, A. K.; Hong, S. J.; Smeltzer, M. S.; Galiano, R. D.; Leung, K. P.; and Mustoe, T. A. (2011) Development of a novel, highly quantitative *in vivo* model for the study of biofilm-impaired cutaneous wound healing. *Wound Repair Regen* 19, 400–410.

(14) Bucalo, B.; Eaglstein, W. H.; and Falanga, V. (1993) Inhibition of cell proliferation by chronic wound fluid. *Wound repair Regen* 1, 181–186.

(15) Kusch, H.; and Engelmann, S. (2014) Secrets of the secretome in *Staphylococcus aureus*. *Int. J. Med. Microbiol.* 304, 133–141.

(16) Gourronc, F. A.; Robertson, M. M.; Herrig, A. K.; Lansdorf, P. M.; Goldman, F. D.; and Klingelutz, A. J. (2010) Proliferative defects in dyskeratosis congenita skin keratinocytes are corrected by expression of the telomerase reverse transcriptase, TERT, or by activation of endogenous telomerase through expression of papillomavirus E6/E7 or the telomerase RNA component, TERC. *Exp. Dermatol.* 19, 279–288.

(17) Tabb, D. L.; Fernando, C. G.; and Chambers, M. C. (2007) MyriMatch: highly accurate tandem mass spectral peptide identification by multivariate hypergeometric analysis. *J. Proteome Res.* 6, 654–661.

(18) Ma, Z. Q.; Dasari, S.; Chambers, M. C.; Litton, M. D.; Sobacki, S. M.; Zimmerman, L. J.; Halvey, P. J.; Schilling, B.; Drake, P. M.; Gibson, B. W.; and Tabb, D. L. (2009) IDPicker 2.0: Improved protein assembly with high discrimination peptide identification filtering. *J. Proteome Res.* 8, 3872–3881.

(19) Larkin, S. M.; Williams, D. N.; Osterholm, M. T.; Tofte, R. W.; and Posalaky, Z. (1982) Toxic shock syndrome: clinical, laboratory, and pathologic findings in nine fatal cases. *Ann. Intern. Med.* 96, 858–864.

- (20) Spaulding, A. R., Salgado-Pabon, W., Merriman, J. A., Stach, C. S., Ji, Y., Gillman, A. N., Peterson, M. L., and Schlievert, P. M. (2014) Vaccination against *Staphylococcus aureus* pneumonia. *J. Infect. Dis.* 209, 1955–1962.
- (21) Schlievert, P. M., Schoettle, D. J., and Watson, D. W. (1979) Purification and physicochemical and biological characterization of a staphylococcal pyrogenic exotoxin. *Infect. Immun.* 23, 609–617.
- (22) Thurlow, L. R., Hanke, M. L., Fritz, T., Angle, A., Aldrich, A., Williams, S. H., Engebretsen, I. L., Bayles, K. W., Horswill, A. R., and Kielian, T. (2011) *Staphylococcus aureus* biofilms prevent macrophage phagocytosis and attenuate inflammation in vivo. *J. Immunol.* 186, 6585–6596.
- (23) Metcalf, D. G., and Bowler, P. G. (2013) Biofilm delays wound healing: A review of the evidence. *Burn Trauma* 1, 5–12.